 DOI: 10.1002/masy.200650514

Simulation of Phase Transitions of Single Polymer Chains: Recent Advances

K. Binder,[1] *J. Baschnagel,*[2] *M. Müller,*[1,3] *W. Paul,*[1] *F. Rampf*[1]

Summary: The behaviour of a flexible polymer chain in solvents of variable quality in dilute solution is discussed both in the bulk and in the presence of an adsorbing wall. Monte Carlo simulations of coarse-grained bead-spring models and of the bond fluctuation model are presented and interpreted in terms of phenomenological theories and scaling concepts. Particular attention is paid to the behaviour of the polymer chain when the temperature of the polymer solution gets lower than the Theta temperature. It is argued that the adsorption transition line at the Theta temperature splits into lines of wetting and drying transitions of polymer globules attached to the wall. In addition, it is shown that the coil-globule transition is followed by a second transition, which in the bond fluctuation model is a crystallization into a regular lattice structure. Performing a finite size scaling analysis on the two transitions it is shown that (for the chosen model) both transitions coincide in the thermodynamic limit, corresponding to a direct collapse of the random coil into the crystal without intermediate coil-globule transition. The implications of this result for the standard mean field or tricritical theory of the coil-globule transition based on a truncated virial expansion are discussed.

Keywords: coil-globule transition; Monte Carlo simulation; polymer adsorption; polymer crystallization; wetting

Introduction

Phase transitions for single polymer chains can occur only in the limit of infinite chain length, $N \to \infty$. Classical problems are the coil-globule transition that occurs when in a dilute polymer solution (monomer volume fraction $\phi \to 0$) the solvent quality varies from good solvent (swollen coils) to bad solvent (collapsed coils) [1–3], or the adsorption transition of a single ''polymer mushroom'' at a wall [4]. Despite much effort, these problems are not fully understood, in particular their interplay (dilute solution of variable solvent quality exposed to an adsorbing wall).[5–13] The present paper presents some simulation results to further elucidate these problems.

First the problem will be introduced and then the coil-globule transition and the further fluid-solid transition [14] of the globule in the bulk solution will be considered, presenting recent results [15] based on the bond fluctuation model [16–18] using the Wang-Landau algorithm [19]. In $d = 3$ dimensions, the surprising finding [15] is that for $N \to \infty$ these two transitions coincide, so the chain directly goes from a (gas-like) coil to the solid structure, the fluid globule disappears. In $d = 2$ dimensions, however, no sharp second transition to a solid structure seems to occur [20].

In presence of a wall, these transitions from coil to globule and solid compete with the adsorption transition of the coil (Figure 1). The standard case considered in the literature [4,21] is that the temperature

[1] Institut für Physik, Johannes Gutenberg Universität Mainz, 55099 Mainz, Staudinger Weg 7, Germany
[2] Institut Charles Sadron, 6, rue Boussingault, F-67083 Strasbourg Cedex, France
[3] Department of Physics, University of Wisconsin-Madison, 1150 University Avenue, Madison WI 53706-1390, USA

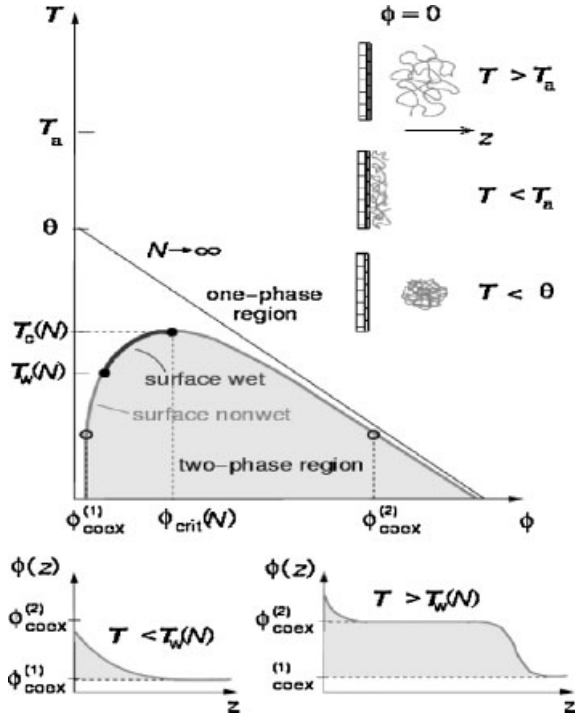

Figure 1.

Schematic phase diagram of a semi-infinite polymer solution (coordinate $z > 0$) with one attractive wall at $z = 0$ plotted in the plane of variables temperature T and volume fraction ϕ taken by the monomers (upper part, left hand side). At temperatures $T < T_c$ (N), there occurs two-phase coexistence (in the shaded region) between a dilute solution (volume fraction $\phi^{(1)}_{coex}$) and a concentrated solution (volume fraction $\phi^{(2)}_{coex}$). The chains in the dilute solution for $N \to \infty$ and $T < \theta$ ($T_c(N \to \infty) \to \theta$) are collapsed (in the limit $N \to \infty$ the coexistence curve degenerates into two straight lines, $\phi^{(1)}_{coex} = 0$, and $\phi^{(2)}_{coex} \propto (\theta - T)$, as indicated). For $\phi = \phi^{(1)}_{coex}$ and $T_w(N) < T < T_c(N)$ formation of a wetting layer occurs, as shown schematically in the lower right part of the diagram. The monomer volume fraction profile $\phi(z)$ vs z is plotted for $T < T_w(N)$, left part, and for $T > T_w(N)$, right part. The shaded area underneath these profiles describes the surface excess Σ: Σ is finite for nonwet surfaces ($T < T_w$), but $\Sigma = \infty$ if the surface is wet. In the phase diagram drawn here it is assumed that the wetting transition is of second order (i.e., there does not occur a prewetting transition line in the one-phase region). In addition, it is assumed that an adsorption transition occurs in the limit $N \to \infty$ at a temperature $T = T_a$ in the good solvent regime ($T > \theta$). For $T < T_a$ the chains are adsorbed on the walls forming pancake-like quasi-two-dimensional configurations, while for $T > T_a$ the chains form non-adsorbed three-dimensional coils near the surface, as they do in the bulk (right upper part). From Metzger et al.[12].

T_a of the adsorption transition exceeds the θ-temperature. But what happens if T_a coincides with θ or even falls below it? One expects there should then be some relation to wetting phenomena [22,23]: remember the θ-temperature is the limiting value of a line of critical points of phase separation between a semi-dilute solution and a dilute solution of collapsed coils occurring in bad solvents (for finite chain length N) [24,25]. As $N \to \infty$, the critical volume fraction $\phi_c(N) \to 0$ and the critical temperature $T_c(N) \to \theta$ (Fig. 1). Note that above some wetting transition temperature $T_w(N)$ the dilute solution will exhibit a wetting layer at the wall. The question arises, how is this behaviour related to the adsorption of single chains in bad solvents? [12]

Of course, there are many motivations to consider such problems: synthetic polymers at surfaces may have important applications as glues or lubricants, and variable

solvent quality always is an issue (e.g., if the solvent is evaporated so the chains are exposed to air, a very bad solvent for polymers); also the present work may be considered as a step towards the modelling of biopolymers at membranes (remember transitions of single proteins such as protein folding). Here we shall not dwell further on applications, but just consider the interplay of energy and entropy that occurs here as a fascinating topic in the statistical mechanics of polymers.

Coil-Globule Transition in the Bulk Versus Crystallization

For this study we use as coarse-grained model for flexible polymers the bond fluctuation model [16–18]. In this model every effective monomer occupies all 8 corners of an elementary cube of the simple cubic lattice, which then are blocked for further occupation. These effective monomers are then connected by effective bonds, whose lengths are not fixed but allowed to vary between 2 and $\sqrt{10}$ lattice spacings. This model has been widely used [26] because it can be simulated rather efficiently, applying moves such as ''random hopping'' of a monomer to a neighboring place on the lattice [16–18], or by applying the ''slithering snake'' or ''pivot'' algorithms [26]. One finds that despite the lattice structure many polymer properties resemble closely those of more realistic off-lattice models, whose simulation is much more costly[26].

To model the variable solvent quality, a square well attraction between monomers of range $\sqrt{6}$ lattice units and strength $\varepsilon = 1$ is used. If we did straightforward Monte Carlo simulations (with the Metropolis acceptance rule [26]) on this problem, one is restricted to [27] $N \leq 150$, because below $T = \theta$ the convergence is very slow, indicating equilibration problems for the collapsed coils. The standard recipe to estimate θ from such simulations is to plot the mean square gyration radius $\langle R_g^2 \rangle$ divided by N versus temperature, because for $T > \theta$ one has [24,28] $\langle R_g^2 \rangle / N \propto N^{2\nu-1} \approx N^{0.18} \to \infty$ as $N \to \infty$, while for $T = \theta$ for the collapsed polymer globules one has instead $\langle R_g^2 \rangle / N \propto N^{-1/3} \to 0$, for $N \to \infty$. Precisely at $T = \theta$ one has $\langle R_g^2 \rangle / N = const$ provided logarithmic corrections [28] are disregarded. In a plot of $\langle R_g^2 / N \rangle$ versus T, using a range of values for N, one roughly finds an intersection point at [27] $\theta \approx 2.02 \pm 0.02$. Of course, knowing that there are logarithmic corrections [28] it may not be a wise strategy to ignore them, this may give rise to severe systematic errors. In fact, using the pruned-enriched Rosenbluth method (PERM) Grassberger [29] succeeded to increase the range of chain lengths up to $N = 600$, and including logarithmic corrections in his analysis yielded [29] $\theta = 2.10 \pm 0.01$. As we shall see below, also this estimate needs to be revised, and one now believes [15] $\theta = 2.18 \pm 0.01$ So even the accurate estimation of the Theta temperature is a problem!

One reason for the difficulties is that for $T < \theta$ and long chains very dense chain configurations occur, which are almost completely ''blocked'' on the ''Monte Carlo time scales'', so the algorithm is not really ergodic in practice, and one needs better algorithms!

This fact became evident when an algorithm invented by Paul and Müller [14] was used, which considers our three-dimensional world as a hyperplane of a four-dimensional thin film. Allowing the monomers to make hops along the additional fourth direction of space, the blocked configurations in the ordinary three-dimensional space now do relax! Of course, for a correct sampling only those configurations can be counted for the Monte Carlo averages, where all monomers are back in the three-dimensional hyperplane again. So this algorithm also needs a lot of computer time and gets difficult for very long chains. Nevertheless, evidence was given [14] that the coil-globule transition at a lower temperature is followed by another transition, of clear first-order nature with a latent heat being present, where the chain forms a crystalline solid phase.

The present work is based on another recently invented [19] powerful algorithm, which is based on the idea to directly sample the density of states g(E). Remem-

ber that the canonical partition function Z(T) can be expressed in terms of g(E) as

$$Z(T) = \sum_E g(E) \exp(-E/k_B T); \quad (1)$$

so if one knows g(E) accurately enough, the problem is solved. One still uses importance sampling, but instead of the standard Metropolis acceptance criterion for a new configuration the Wang-Landau method [19] uses as a transition probability

$$\text{prob}(\text{old} \to \text{new}) = \text{Min}\{1, g[E(\text{old})]/g[E(\text{new})]\} \quad (2)$$

The idea of the algorithm is to perform a random walk through configuration space by using the above ordinary Monte Carlo moves and record the number of configurations H(E) visited for given energy values E. One uses an iteration procedure: Starting with the arbitrary choice of $g(E) = 1$ for all E, one modifies g(E) to fg(E) after the Monte Carlo move that has resulted in a visit to a state with energy E. At the beginning, the choice $f = e^1$ is made. This is continued, using Eq. (2), until the monitored histogram of visits H(E) is sufficiently flat. Then one sets $H(E) = 0$ for all E again, and repeats the sampling with a new choice for f, namely $f_{new} = \sqrt{f_{old}}$. By "sufficiently flat" we require in practice that the number of visits to any state is a least 80% of the average number over visits for all states. For $f \to 1$ the method fulfils detailed balance, and the measured density of states g(E) converges to the exact one. This method has already been proven very useful for many models [30].

For our model the energy falls in the interval $[E_{min}, 0]$ with $-5N < E_{min} < -4N$. We performed simulations for subintervals of this range of typical widths 100–200, where adjacent subintervals had an overlap equal to half their widths. Results for g(E) in these overlap regions from different subintervals typically agree within a relative accuracy of 10^{-6} to 10^{-5}. For $N = 128$, we performed 10 independent determinations of $\ell n[g(E)]$ and found that the maximum relative deviation never exceeded 10^{-4}.

In this way it is possible to sample a g(E) that spans an enormously large range (note that for $N = 512$ $\ell n[g(E)]$ spans a range of about 900 already, see Fig. 2). Note that g(E) can only be obtained up to some undetermined constant factor: so we have chosen the arbitrary normalization $g_N(E = 1) = 1$ for all N, but for the computation of observables such as the specific heat this normalization constant does not matter.

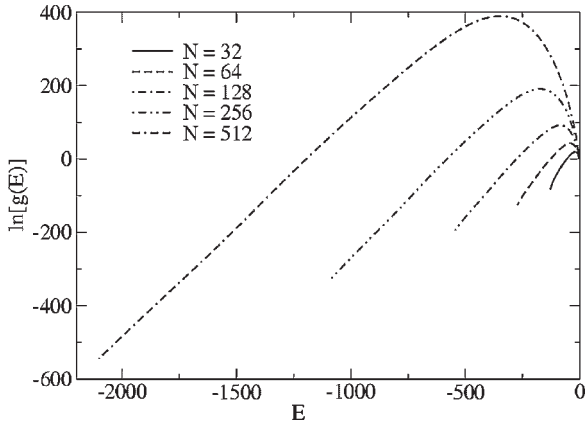

Figure 2.
Logarithm of the density of states for polymer chains described by the bond fluctuation model with an attractive energy $\varepsilon = 1$ of range $\sqrt{6}$ between monomers, for chain lengths N in the range $32 \le N \le 512$. From Rampf et al. [15].

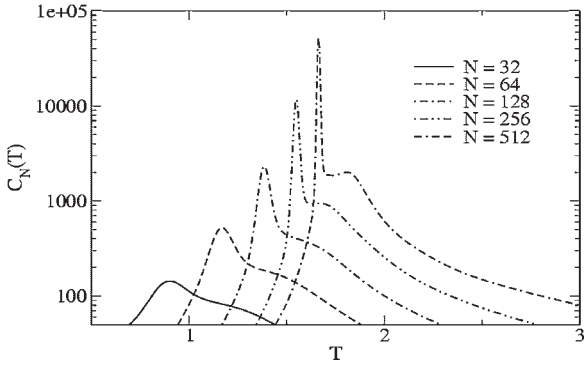

Figure 3.
Specific heat plotted vs. temperature for various chain lengths, as indicated. Note the logarithmic ordinate scale. From Rampf et al.[15].

The specific heat is easily obtained from Eq. (1) via the fluctuation relation

$$\mathbf{C_N(T)} = (\langle E^2 \rangle - \langle E \rangle^2)/T^2 \qquad (3)$$

One sees (Fig. 3) that a broad peak starts to develop already at rather high temperatures and on top of this peak a rather sharp second peak grows, developing into a delta function for $N \to \infty$. This peak is connected with a crystallization transition in our model.

The crystalline state reached at temperatures below this liquid-solid transition is still rather disordered, as far as the orientations of the effective bonds are concerned (Fig. 4a). However, if we do not display the bonds at all, but rather draw spheres around the centers of mass of all monomers, then we clearly recognize that there is crystalline order really present, with a cubic structure. Due to the underlying simple cubic lattice, the structure must be commensurate with this lattice. However, the favoured structure is neither simple cubic nor body-centered cubic or face-centred cubic, at least for the accessible values of N. Rather one finds [20] a modified hexagonal-like packing with a layer sequence ACBC, where the subsequent double-layers AC and BC are turned with respect to each other by 90 degrees.

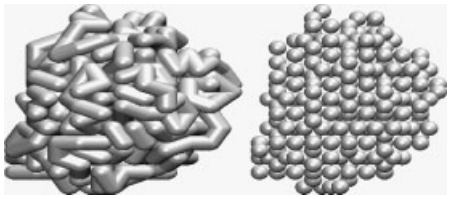

Figure 4.
a) Snapshot picture of a crystallized chain of length N = 512 with an energy per monomer of E ≈ - 5.2 forming a solid globular state. Bonds are presented as cylinders b) Same as a, but displaying the monomers (shown as spheres) omitting the bonds between them. From Rampf [20] (=Figure 4.25 ± 4.26, right part).

This first order transition, which has a latent heat of about [15] $\Delta U/N = 1.8 \pm 0.2$, means that there occurs two-phase coexistence between liquid and solid phases at the transition temperature. Of course, for finite N this transition is rounded by finite size, but its location can be found rather accurately by the "equal weight rule" [30]. The density profiles around the center of mass of the globule at phase coexistence are shown in Fig. 5. Note that the widths of the interface between the fluid phase and surrounding gas increases much stronger with N than the corresponding width for the crystal-gas interface. As it must be, the density in the crystal interior is high and independent of chain length; in the fluid phase, the density $\rho_{liquid}(N)$ is lower and systematically decreases with increasing N. Actually this decrease can be fitted to a power law, $\rho_{fluid} \propto N^{-0.153}$. However, the exponent of this power law is not in accord with the theoretical prediction. Using the

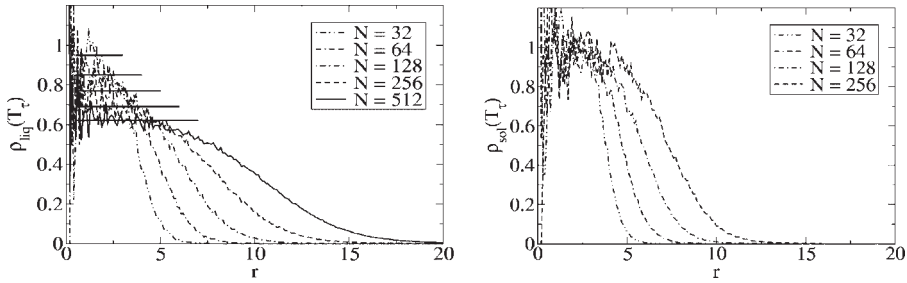

Figure 5.
Radial density profile at phase coexistence for the fluid globule (upper part) and the solid globule (lower part), for chain length from N = 32 to N = 512, as indicated. Note that in the solid phase the density in the globule interior is independent of N, while in the fluid phase the density decreases systematically with increasing N, as indicated by the horizontal straight lines. From Rampf [20].

crossover scaling description of the coil-globule transition[1–3,24] for the mean square gyration radius

$$\left\langle R_g^2 \right\rangle^{1/2} = N^{1/2} f_{\pm}(N\tau^2), \qquad \tau \equiv 1 - T/\theta \tag{4}$$

and the condition that for $T < \theta$ the scaling function f_(x) behaves as f_(x) $\propto \times^{-1/6}$ for $x \to \infty$ one concludes that $\left\langle R_g^2 \right\rangle^{1/2} \propto (N/\tau)^{1/3}$ for large N and thus the volume V taken by the globule scales as $V \propto \left\langle R_g^2 \right\rangle^{3/2} \propto N/\tau$, implying that the liquid density is $\rho_{liquid} = N/V \propto \tau$. Since as we shall show below, the distance τ_{tr} of the liquid-solid transition from the Theta temperature scales as $\tau_{tr} \propto N^{-1/3}$, one would predict $\rho_{liquid} \propto N^{-1/3}$ as well, at variance with the observation.

Fig. 6 presents our results for the shift of the coil-globule and liquid-solid transitions with chain length N. For the coil-globule transition one expects from the standard theory [1–3,24] that

$$T_\theta(N) = \theta - a_1/\sqrt{N} + a_2/N + - \ldots, \tag{5}$$

where a_1, a_2 are constants. For the crystallization transition, however, we expect that the shift of the transition is due to surface

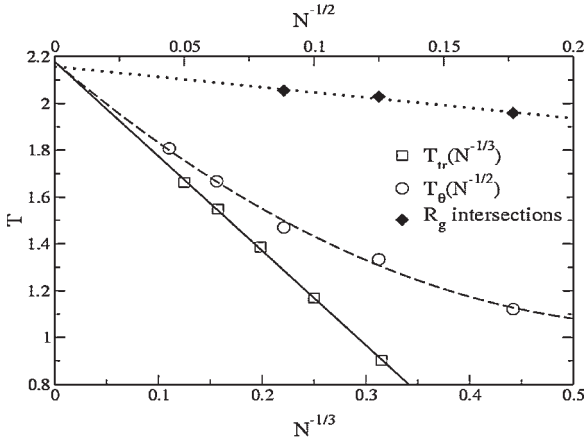

Figure 6.
Chain length dependence of the temperature of the specific heat peak for the coil-globule transition (open circles) and for the liquid-solid transition (open squares). The former are plotted vs. $N^{-1/2}$ (scale on top) and the latter vs. $N^{-1/3}$ (scale on bottom). The filled diamonds are estimates for the coil globule transition temperature from intersections of $R_g^2(T)/N$ versus T curves for chain lengths N and 2N, assigned to chain length N, and plotted vs. $N^{-1/2}$ (scale on top). The fit curves are discussed in the text. From Rampf et al.[15].

effects, and since the relative importance of the surface free energy of the crystallite relative to its bulk free energy should decrease as $N^{-1/3}$, we expect for the transition temperature a relation

$$T_{tr}(N) = T_{crys} - b_1/N^{1/3} + - \ldots \quad (6)$$

The data (Fig. 6) indeed are compatible with such extrapolations, but surprisingly we find that in the limit $N \to \infty$ the crystallization temperature T_{crys} coincides with the Theta temperature θ! So in the limit of very long chains the temperature region where the fluid globule exists becomes vanishingly small. We have no convincing explanation why this happens for our model, and we do not know to what extent this is a general feature of all polymers or only a specific property of our model. Of course, for off-lattice models we expect a glassy solid rather than a crystal, and there exists preliminary simulation evidence in favour of this globule-glass transition[31], but otherwise the problem whether or not these two transitions coincide for $N \to \infty$ remains.

Here we also comment on the problem of locating the Theta point via intersections of $\langle Rg2/N \rangle$ vs. T curves. On a very expanded temperature scale, it looks as if a well-defined intersection point slightly above $T = 2$ is present, as claimed by Wilding et al. [27] (Fig. 7). Zooming in by expanding the scales, however, we see that the intersection points shift systematically to higher temperature the larger N. Extrapolating successive intersections is compatible with our estimate $\theta = 2.18 \pm 0.01$ (Fig. 6).

Such data for the gyration radius or end-to-end distances are also obtained from Wang-Landau sampling, recording [15,20] in each configuration X_E of the final histogram H(E) the corresponding observable $R_g^2(X_E)$, and thus

$$\overline{R}_g^2(E) = [1/H(E)] \sum_{X_E=1}^{H(E)} R_g^2(X_E) \quad (7)$$

In this way, more precise data than by Metropolis sampling [27] could be obtained. [15]

Being interested in the interplay of collapse and adsorption (Fig. 1) we have repeated this study for two-dimensional polymers [20] (this case is appropriate if $T_a \gg \theta$). No clear signal of two distinct transitions as yet could be observed, however. Extrapolating the position of the specific heat peaks is compatible with a preliminary estimate for the Theta

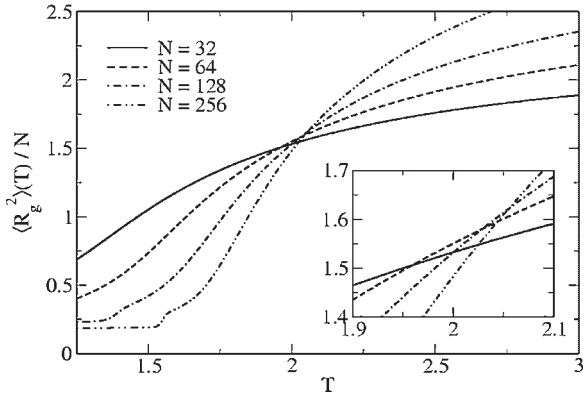

Figure 7.
Mean-square radius of gyration divided by chain length as a function of temperature, including chain lengths from $N = 32$ to $N = 256$. The apparent intersection point yields a rough estimate of the coil globule transition temperature. A closer look (insert) shows, however, that all intersection points shift systematically towards higher temperature the larger the chain length. Note also for $N = 256$ the rounded step near $T = 1.55$, signifying the crystallization transition. From Rampf et al.[15].

temperature $\theta = 1.30 \pm 0.05$ in $d = 2$ dimensions. More work is still necessary to clarify this problem, however.

Chain Collapse Versus Chain Adsorption

Finally, we discuss the problem posed in Fig. 1, when both energy scales ε for the collapse and ε_w for adsorption become comparable. We discuss this problem in terms of a qualitative three-dimensional diagram (Fig. 8) with inverse adsorption energy $\tilde{\varepsilon}_w^{-1}(\tilde{\varepsilon}_w = \varepsilon_w/T)$ and inverse energy between monomers $\tilde{\varepsilon}^{-1}(\tilde{\varepsilon} = \varepsilon/T)$ and the volume fraction ϕ of the monomers in solution as variables. The adsorbed chains exist in the limit $N \to \infty$ to the right of the broken line in the $\phi = 0$ plane, for $T > \phi$. For finite chain lengths, there are transitions at finite concentrations below the critical temperature $T_c(N)$, and at the coexistence curves of these phase separations there occur wetting and drying transitions, if the solution is exposed to a wall. These transitions can be critical (second order), first order, or tricritical. When the chain length N goes to infinity, the critical temperature of phase separation moves into the Theta temperature, the coexistence curve tends into two straight lines. Then also the tricritical wetting or drying transitions must converge into the Theta temperature at the adsorption transition point. This consideration indicates that at the Theta temperature the structure of adsorbed chains will change. A nonadsorbed ''mushroom'' at the Theta tempera-

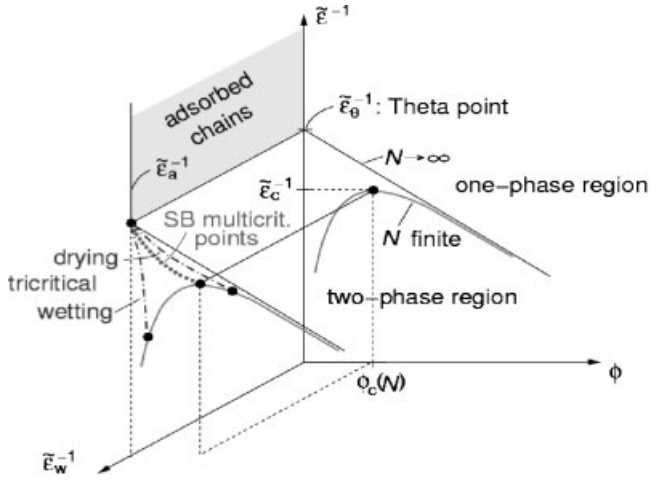

Figure 8.

Conjectured global phase diagram of adsorption and tri-critical wetting transitions of polymer solutions. Parameters chosen are the normalized interaction energy between monomers in the bulk, $\tilde{\varepsilon} = \varepsilon/T$, and a normalized short-range monomer-wall interaction, $\tilde{\varepsilon}_w = \varepsilon_w/T$, and the monomer volume fraction in the solution. The adsorption transition occurs only for $N \to \infty$ in the plane $\phi = 0$, for $\tilde{\varepsilon}_w = \varepsilon_a(\tilde{\varepsilon})$, which is approximated as a straight line here (for $\tilde{\varepsilon} < \tilde{\varepsilon}_0$, i.e. temperatures higher than the Theta temperature). The part of the plane, $\phi = 0$, $\tilde{\varepsilon} < \tilde{\varepsilon}_\theta$, where from a dilute solution chains get adsorbed in a quasi-two-dimensional configuration, is shown as a shaded area. For $\tilde{\varepsilon} < \tilde{\varepsilon}_\theta$ phase separation in the bulk occurs. The bulk phase diagram does not depend on $\tilde{\varepsilon}_w$, of course. For $N \to \infty$ the polymer-rich phase boundary in the $\tilde{\varepsilon}^{-1} - \phi$ plane is simply a straight line $\phi \propto 1 - T/\theta$ ending in the Theta point, while the phase boundary poor in polymers simply is the ordinate axis ($\phi = 0$) in that plane. For finite N, phase separation occurs only of $\tilde{\varepsilon}$ exceeds $\tilde{\varepsilon}_c$ which corresponds to $T_c(N)$ in Fig. 1, and there is a nonzero critical volume fraction $\phi_c(N)$. For this Ising-type phase transition in the bulk, on the surface one expects a surface-bulk (SB) multicritical point if surface fields (coupling linearly to the order parameter of the transition) vanish, while for nonzero surface fields wetting transitions occur. These wetting transitions can be of first order, second order, or tricritical; one expects that the tricritical wetting/drying transitions merge with the line of SB transitions at the Theta point at the adsorption transition, since the latter also is a SB multicritical point in the field-theoretic description. From Metzger et al.[12].

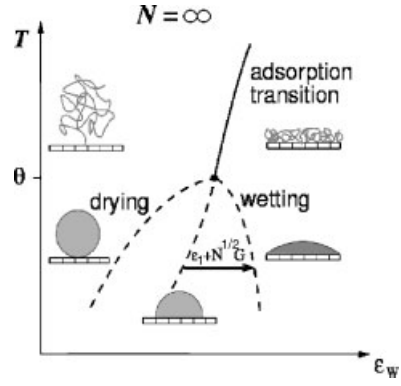

Figure 9.
Phase diagram in the limit $N \to \infty$ as a function of the temperature T and the monomer wall attraction ε_w (schematic). The line of adsorption transitions approaches the θ-temperature without singularity. From Metzger et al.[12].

ture will transform into a globule touching the surface at the anchoring point of this end-grafted polymer chain (Fig. 9), an adsorbed "pancake" will transform into a much denser wetting layer. The adsorption transition at the Theta temperature should then split into two transitions, drying and wetting transitions: in between we predict states of incomplete wetting. We speculate that the infinitely long chain in this region may resemble a sphere-cap shaped droplet attached to the wall (Fig. 9). Note that in Fig. 9 we have allowed for a dependence of the adsorption threshold on T/ε, although no such dependence could be detected in numerical studies so far [8].

So far, we have taken only modest first step towards studying this problem sketched in Fig. 9, using an off-lattice bead-spring model [32]. Nonbonded beads interact with Lennard-Jones forces,

$$U_{LJ}(r_{ij}) = 4\varepsilon\left[(\sigma/r_{ij})^{12} - (\sigma/r_{ij})^{6}\right] + C, \quad r \le r_c = 2.2^{1/6}\sigma, \tag{8}$$

while $U_{LJ}(r_{ij} > r_c) = 0$, and the constant C is chosen such that $U_{LJ}(r_{ij} = r_c)$ is continuous.

Between bonded atoms there acts in addition the finitely extensible nonlinear elastic (FENE) potential,

$$U_{FENE}(r_{ij}) = -\frac{1}{2}KR_0^2 \ell n\left(1 - \frac{r_{ij}^2}{R_O^2}\right), \quad r_{ij} < R_0, U_{FENE}(r_{ij} > R_0) = \infty, \tag{9}$$

where $K = 30$, $R_0 = 1.5$ (choosing units $\varepsilon = 1$, $\sigma = 1$. This choice ensures that the potential minimum for bonded neighbors along the chains occurs for $r_{min} = 0.96$, while for nonbonded ones it occurs for $r_{min} = 2^{1/6} \approx 1.13$. Due to the misfit between these two distances no crystal formation is found at low temperatures, rather the system freezes into a glassy state [32]. This transition occurs at a very low temperature, $T_{glass} \approx 0.4$, far below the Theta temperature ($\theta \approx 3.3 \pm 0.2$)[33] leaving a broad range of $T < \theta$ accessible for our simulations.

As a first step, the adsorption transition in this model has been studied carefully, [12], using a wall potential

$$U_w(z) = \varepsilon_w[z^{-9} - fz^{-3} + (D - z)^{-9}], \quad f = 100, \tag{10}$$

using a box geometry $L \times L \times D$ with one attractive wall at $z = 0$ and a purely repulsive wall at $z = D$, with box sizes up to $L = 500$, $D = 500$ (and periodic boundary conditions in x and y directions). Note that Eq. (10) can be interpreted as resulting from integrating over a standard 12 – 6 Lennard-Jones potential over a half space. Due to the choice of the parameter f $U_w(z)$ has its minimum at about $z_{min} \approx 0.57$.

Choosing $T = 4$, slightly above $T = \theta$, the adsorption transition has been located in two ways: (i) from a scaling analysis of the linear dimensions of the adsorbed chain (ii) from a scaling analysis of the surface excess defined from the density profile $\phi(z)$ of the solution as

$$\rho_s = \int_0^{D/2} [\phi(z) - \phi_{bulk}]dz/N \tag{11}$$

It was found [12] that for $N \to \infty$ the surface excess changes sign at the adsorption transition, which occurs at $\varepsilon_a = 0.00938 \pm 0.00026$ (Fig. 10). Note that ρ_s is expected to

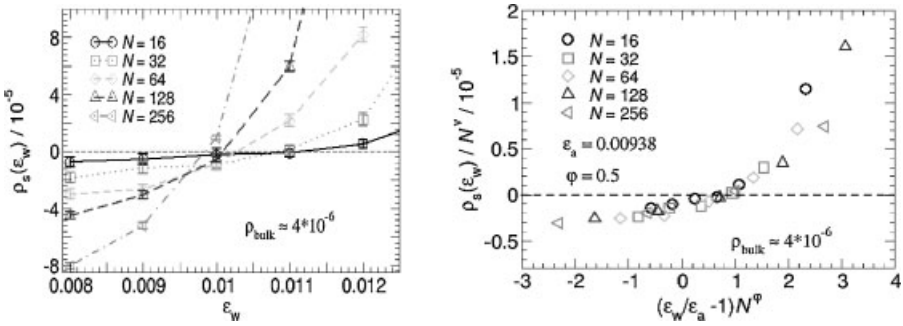

Figure 10.
a) Surface excess density (ρ_s plotted vs. ε_w. for a bulk density $\rho_{bulk} = 4 \times 10^{-6}$ and several choices of N as indicated. b) Scaling plot of the surface excess ρ_s vs the scaled distance $(\varepsilon_w/\varepsilon_a - 1)N^{\varphi}$ for a choice $\varphi = 0.5$ for the crossover exponent, $\varepsilon_a = 0.00938$, and five different values of N. From Metzger et al.[12].

diverge to $+\infty$ ($-\infty$) if a wetting (drying) transition occurs. It remains to carry out studies as shown in Fig. 10 for $T < \theta$, however. Thus verification of the speculative predictions shown in Figs. 8, 9 is still open.

Discussion

The phase behavior of single polymer chains in bulk solution or end-grafted at walls is still purely understood. While in the limit where the chain length $N \to \infty$ three phases occur, analogous to the three phases gas, liquid, solid of bulk matter, namely the swollen coil $\left(\langle R_g^2 \rangle \propto N^{2\nu}\right)$ with $\nu \approx 0.59$), the collapsed fluid globule $\left(\langle R_g^2 \rangle \propto N^{2/3}\right)$ and the solid (crystalline or glassy) state, the nature of the transition between these states in bulk solution still seems incompletely understood. For chains end-grafted at walls these transitions compete with the adsorption transition, if an attractive interaction between the monomers and the wall is present. Under bad solvent conditions, a relation to wetting phenomena is predicted, but a full understanding of the global phase diagram is still lacking.

Acknowledgements: One of us (F. R.) acknowledges financial support from the Deutsche Forschungsgemeinschaft (DFG) under grant N° SFB 625/A3, another (S.M.) under grant No Ba 1554, a third (M.M.) via a Heisenberg fellowship. Furthermore this research has profited from support from the European Science Foundation (ESF) via the SUPERNET program and from INTAS project 01-607. Helpful discussions with E. Eisenriegler, P. Grassberger, A. Yu. Grosberg and D. P. Landau are acknowledged as well.

[1] I. M. Lifshitz, A. Y. Grosberg, A. R. Khoklov, *Rev. Mod. Phys.* **1978**, *50*, 683.
[2] A. Y. Grosberg, A. R. Khoklov, *Adv. Polym. Sci.* **1981**, *53*.
[3] A. Y. Grosberg, A. R. Khoklov, "*Statistical Physics of Macromolecules*", AIP Press, New York 1994.
[4] E. Eisenriegler, "*Polymers Near Surfaces*", World Scientific, Singapore 1993.
[5] A. R. Veal, J. M. Yeomans, G. Jug, *J. Phys. A* **1991**, *24*, 827.
[6] T. Vrbova, S. G. Whittington, *J. Phys. A* **1996**, *29*, 6253.
[7] T. Vrbova, S. G. Whittington, *J. Phys. A* **1998**, *31*, 3989.
[8] T. Vrbova, K. Prochazka, *J. Phys. A* **1999**, *32*, 5469.
[9] Y. Singh, D. Giri, S. Kumar, *J. Phys. A* **2001**, *34*, L67.
[10] R. Rajesh, D. Dhar, D. Giri, S. Kumar, Y. Singh, *Phys. Rev. E* **2002**, *65*, 056124.
[11] P. Mishra, S. Kumar, Y. Singh, *Physica* **2003**, *323*, 453.
[12] S. Metzger, M. Müller, K. Binder, J. Baschnagel, *J. Chem. Phys.* **2003**, *118*, 8489.
[13] J. Krawczyk, A. L. Owczarek, T. Prellberg, A. Rechnitzer, *Europhys. Lett.* **2005**, *70*, 726.
[14] W. Paul, M. Müller, *J. Chem. Phys.* **2001**, *195*, 630.
[15] F. Rampf, W. Paul, K. Binder, *Europhys. Lett.* **2005**, *70*, 628.

[16] I. Carmesin, K. Kremer, *Macromolecules* **1988**, *21*, 2819.
[17] H. P. Deutsch, K. Binder, *J. Chem. Phys.* **1991**, *94*, 2294.
[18] W. Paul, K. Binder, D. W. Heermann, K Kremer, *J. Phys. II* **1991**, *1*, 37.
[19] F. Wang, D. P. Landau, *Phys. Rev. E* **2001**, *64*, 056101.
[20] F. Rampf, *Dissertation*, Johannes Gutenberg Universität, Mainz 2005.
[21] E. Eisenriegler, K. Kremer, K. Binder, *J. Chem. Phys.* **1982**, *77*, 6296.
[22] I. Schmidt, K. Binder, *J. Phys. (Paris)* **1985**, *46*, 1631.
[23] S. Dietrich, in: "*Phase Transitions and Critical Phenomena, Vol. 12*" C. Domb, J. L. Lebowitz, eds. Academic, New York 1988, p. 1.
[24] P. G. de Gennes, "*Scaling Concepts in Polymer Physics*" Cornell University Press, Ithaca, 1999
[25] B. Widom, *Physica A* **1993**, *194*, 523.
[26] K. Binder, ed. "*Monte Carlo and Molecular Dynamics Simulations in Polymer Science*" Oxford Univ. Press, New York 1995.
[27] N. B. Wilding, M. Müller, K. Binder, *J. Chem. Phys.* **1996**, *105*, 802.
[28] L. Schäfer "*Excluded Volume Effects in Polymer Solutions as Explained by the Renormalization Group*" Springer, Berlin 1999.
[29] P. Grassberger, *Phys. Rev. E* **1997**, *56*, 3682.
[30] D. P. Landau, K. Binder "*A Guide to Monte Carlo Simulations in Statistical Physics, 2nd ed.*" Cambridge Univ. Press, Cambridge, 2005.
[31] A. Milchev, K. Binder, *Europhys. Lett.* **1994**, *26*, 671
[32] C. Bennemann, W. Paul, K. Binder, B. Dünweg, *Phys. Rev. E* **1998**, *57*, 843.
[33] M. Müller, L. G. MacDowell, *Macromolecules* **2000**, *33*, 3902.

